New Insights on Atomic-Resolution Frequency-Modulation Kelvin-Probe Force-Microscopy Imaging of Semiconductors

Sascha Sadewasser,[1] Pavel Jelinek,[2] Chung-Kai Fang,[3] Oscar Custance,[3,*] Yusaku Yamada,[4] Yoshiaki Sugimoto,[4] Masayuki Abe,[4] and Seizo Morita[4]

[1]*Helmholtz Zentrum Berlin für Materialien und Energie, Hahn-Meitner-Platz 1, Berlin, Germany*
[2]*Institute of Physics, Academy of Sciences of the Czech Republic, Cukrovarnicka 10, Prague, Czech Rebublic*
[3]*National Institute for Materials Science (NIMS), 1-2-1 Sengen, Tsukuba, Ibaraki, Japan*
[4]*Graduate School of Engineering, Osaka University, 2-1 Yamada-Oka, Suita, Osaka, Japan*

(Received 9 September 2009; published 28 December 2009)

We present dynamic force-microscopy experiments and first-principles simulations that contribute to clarify the origin of atomic-scale contrast in Kelvin-probe force-microscopy (KPFM) images of semiconductor surfaces. By combining KPFM and bias-spectroscopy imaging with force and bias-distance spectroscopy, we show a significant drop of the local contact potential difference (LCPD) that correlates with the development of the tip-surface interatomic forces over distinct atomic positions. We suggest that variations of this drop in the LCPD over the different atomic sites are responsible for the atomic contrast in both KPFM and bias-spectroscopy imaging. Our simulations point towards a relation of this drop in the LCPD to variations of the surface local electronic structure due to a charge polarization induced by the tip-surface interatomic interaction.

DOI: 10.1103/PhysRevLett.103.266103 PACS numbers: 68.35.bg, 07.05.Tp, 68.37.Ps

The work function is a property of solids with fundamental relevance, among others, in photovoltaic energy conversion technology [1]. This magnitude describes the energy required to extract an electron from a material and bring it to infinity [2,3], and in the case of semiconductors it is generally regarded as the energy difference between the Fermi level and the local vacuum level [1]. The work function can be measured by thermionic emission, photoemission spectroscopy or Kelvin-probe force microscopy (KPFM) [4]. The latter technique measures variations of the contact potential difference (CPD) between a surface and the probe of an atomic force microscope (AFM), which originates from a disparity in their respective work functions [5]. KPFM is widely applied to characterize local variations of the work function on a wide variety of material surfaces [6–11] down to the nanometer scale [12], and very recently also to characterize the charge state of individual atoms [13].

Although the work function is considered a macroscopic concept, founded on the crystalline arrangement, the electronic properties, local structure, and composition of the surface, several authors have reported KPFM images showing variations of the CPD at atomic scale on semiconductors [14–17] and insulators [18]. The origin of this atomic contrast in the local contact potential difference (LCPD) [19] is still not fully understood, existing a strong controversy between several hypotheses. In the case of ionic crystals, an origin based on short-range electrostatic forces due to the variations of the Madelung surface potential has been suggested [18], yet an induced polarization of the ions at the tip-surface interface due to the bias voltage modulation applied in KPFM may be an alternative contrast mechanism [20]. In the case of semiconductor surfaces, some authors attribute atomic resolution in KPFM images to possible artifacts [16,21].

In this Letter, we provide new evidence on the phenomenology of atomic-scale KPFM imaging on semiconductor surfaces by means of a thoughtful set of experiments performed over the same surface area with identical tip-apex termination. By combining this rich experimental information with first-principles calculations, we propose an alternative mechanism for atomic-scale contrast in LCPD images on semiconductors.

The experiments were performed with an ultrahigh-vacuum low-temperature AFM operated under the frequency modulation detection method [22], keeping the cantilever oscillation amplitude constant, and using a fully digital AFM controller [23]. The measurements were carried out at a tip and sample temperature of 77 K on a Si(111)-(7×7) surface with a low concentration of substitutional Pb atoms. For details about tip and sample preparation, see [24]. For topographic imaging, the electrostatic long-range interaction was minimized by compensating the CPD at a tip-surface separation of 5 nm [25]. Spectroscopy acquisition and tip-surface short-range (SR) force quantification [26,27] is described in [24]. Density functional theory (DFT) simulations of vertical scans of a well-tested Si tip model [28] over the atoms of a Pb/Si(111)-(7×7) surface were performed using the FIREBALL code [29]. The surface was modeled by a slab of 7 Si layers with H saturating the deeper Si layer. At each step of the simulation, the atoms were allowed to relax to minimize the total energy of the system with convergence criteria in energy and force of 10^{-6} eV and 0.05 eV/Å, respectively. The surface Brillouin zone was sampled with the Γ k point. For more details about the simulations, see [24].

In KPFM, a small ac-bias voltage (V_{ac}) at the frequency f_{ac} is added to the dc-bias voltage (V_s) applied between tip and surface, resulting in an oscillating component of the electrostatic force (F_{el}):

$$F_{el} = -\frac{1}{2}\frac{\partial C}{\partial Z}[V_s - V_{CPD(LCPD)} + V_{ac}\sin(2\pi f_{ac} t)]^2, \quad (1)$$

where $\frac{\partial C}{\partial Z}$ is the derivative of the tip-sample capacitance determined by the geometry. A feedback controller is then used to adjust the value of V_s to match $V_{CPD(LCPD)}$ for every tip position, minimizing F_{el} and ideally providing a measurement of the LCPD [4].

Okamoto *et al.* [16] suggested that the ac component of F_{el} may produce variations of the tip-surface separation (Z) so that the AFM tip could probe a varying part of the SR interaction at close enough distances during each oscillation cycle, yielding to a SR contribution to the f_{ac} component of the frequency shift (Δf) that might be followed and compensated by the KPFM controller. This effect could consequently produce atomic contrast in the KPFM signal as an artifact. Another hypothesis to explain atomic-scale variations of the LCPD in semiconductors is based on the observation of a peaklike increase of the Δf at bias voltages around the CPD value [19,21] that has been attributed to resonant tunneling between electronic states of tip and surface [21]. This deviation from a parabolic dependence of Δf on V_s may influence the performance of the KPFM controller, resulting in a spurious atomic contrast in the LCPD.

In almost all the measurement sessions we have undertaken to elucidate atomic contrast in the LCPD on semiconductors [30], we started by imaging the same surface area using standard KPFM and bias-spectroscopy imaging, at several tip-surface separations around the onset of the SR interaction force. For KPFM imaging, the induced oscillation on the Δf due to the ac component of the bias voltage was analyzed by a lock-in amplifier and further compensated by a KPFM controller for each tip lateral position [14]. Bias-spectroscopy imaging was performed by measuring a $\Delta f(V_s)$ curve over each pixel of a topographic image, controlling the AFM tip height at the topographic set point (Δf_{SP}) before the curve acquisition. These $\Delta f(V_s)$ curves were then individually fitted to a parabolic dependence to obtain the voltage V^* that minimizes the electrostatic interaction—another way to measure the LCPD [13,25]. Thus, this procedure yields a map of the LCPD that can be correlated with both topography and KPFM images [31]. Figure 1 summarizes the results of probing the same surface area with identical tip apex using these two imaging modes. The topography reveals the typical appearance of the Pb/Si(111)-(7 × 7) surface, showing the substitutional Pb adatoms as higher protrusions [Figs. 1(a) and 1(c)] [32]. Interestingly, both the bias-spectroscopy [Fig. 1(b)] and the KPFM [Fig. 1(d)] images display similar atomic contrast, with a lower LCPD above the Si and the substitutional Pb adatoms, and slightly

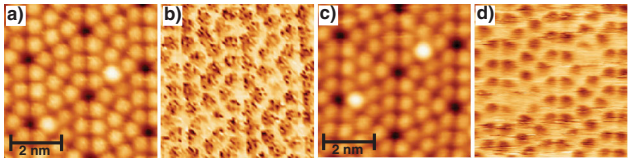

FIG. 1 (color online). (a) Topographic image of an area of the Si(111)-(7 × 7) surface with substitutional Pb adatoms (brighter protrusions) measured on a 64 × 64 pixel grid, and (b) simultaneously obtained bias-spectroscopy image (see text for details). (c) Topography and (d) simultaneously measured KPFM image at the same surface location shown in (a) on a 256 × 256 pixel grid. The Δf_{SP} for (a) and (c) were −9.4 and −8.6 Hz, respectively; both were measured at $V_s = 180$ mV. Bright (dark) contrast in (b) and (d) correspond to 66.8 mV (−470 mV) and 55.5 mV (− 342.7 mV), respectively. KPFM and AFM parameters were $V_{ac} = 0.5$ V, $f_{ac} = 1$ kHz, free-oscillation cantilever fundamental resonance frequency (f_0) 161 372.0 Hz, cantilever oscillation amplitude (A) 93 Å , and cantilever stiffness 30 N/m.

higher signal over the Si adatoms with depleted charge due to the presence of the Pb adatoms [33] and over the corner holes of the Si(111)-(7 × 7) surface [34]. Quantitatively, slightly lower LCPD values are obtained for the KPFM image, possibly due to a faintly larger tip-surface separation due to the additional ac bias.

To gather more information, we also independently performed force [26] and bias-distance spectroscopic experiments [i.e., $\Delta f(Z)$ curves and $\Delta f(V_s, Z)$ maps] above specific atomic sites. Figure 2(a) shows one of these $\Delta f(V_s, Z)$ maps acquired over the Si corner adatom marked on the inset image in Fig. 3(a). In these maps, a vertical line profile provides a $\Delta f(Z)$ curve at a given V_s, while a horizontal line profile offers a bias-spectroscopy curve [$\Delta f(V_s)$] at a specific tip-surface separation. A parabolic dependence of these $\Delta f(V_s)$ curves is clearly observed [Fig. 2(b)] and can be fitted (gray lines) to extract the evolution of the voltage that minimizes the electrostatic

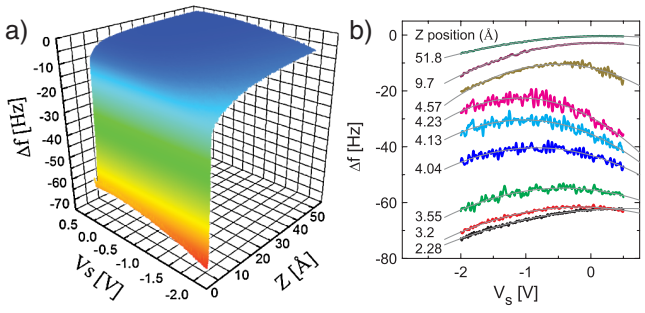

FIG. 2 (color online). (a) $\Delta f(V_s, Z)$ map measured over the Si corner adatom pointed in the inset of Fig. 3(a). (b) Bias-spectroscopy curves extracted from (a) at several tip-surface separations with parabolic fits (gray lines) to extract the bias voltage that minimizes the tip-surface electrostatic interaction (V^*). Acquisition parameters are the same as in Fig. 1.

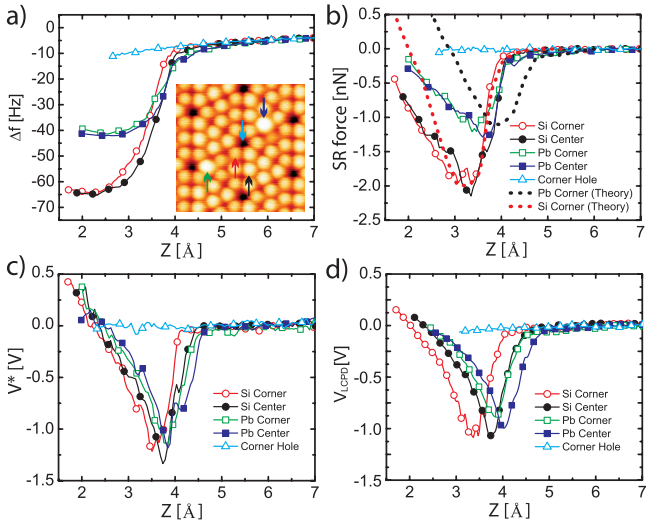

FIG. 3 (color online). (a) $\Delta f(Z)$ curves extracted from $\Delta f(V_s, Z)$ maps measured over the atomic positions marked with arrows in the inset topography image, quantifying the Δf at minimum electrostatic interaction for each tip-surface separation [$\Delta f(V_s = V^*, Z)$]. The color code for arrows and plot lines is the same. (b) Short-range interaction force obtained from the $\Delta f(Z)$ curves in (a). (c) Variation of V^* with the tip-surface separation obtained from the $\Delta f(V_s, Z)$ maps mentioned in (a). (d) Variation of V_{LCPD} with the tip-surface separation obtained from individual $\Delta f(Z)$ curves acquired over the same atomic positions using an active KPFM feedback to minimize the electrostatic interaction at each point of the curve. Acquisition parameters are the same as in Fig. 1.

interaction as a function of the tip-surface separation [$V^*(Z)$] above the surface atom.

Figure 3 summarizes a comparison of several spectroscopic measurements over various atomic positions of the same surface area as in Fig. 1. Figure 3(a) displays $\Delta f(Z)$ curves obtained from $\Delta f(V_s, Z)$ maps acquired over the atoms pointed by arrows in the inset image. The values of these $\Delta f(Z)$ curves quantify the Δf at minimum electrostatic interaction for each tip-surface separation, i.e., $\Delta f(V_s = V^*, Z)$, obtained from parabolic fits to the horizontal line profiles of the corresponding $\Delta f(V_s, Z)$ map. The SR forces obtained from these $\Delta f(Z)$ curves and the corresponding variation of V^* with the tip-surface separation are displayed in Figs. 3(b) and 3(c), respectively. Surprisingly, $V^*(Z)$ shows a considerable drop at the onset of the SR force from an almost constant value of $\sim$180 mV away from the surface (see Fig. S1 at [24]) down to -1.25 V near the region of the maximum attractive SR force. Similar behavior is attained when performing force spectroscopy over the same atoms with identical tip-apex termination but compensating the LCPD at each point of the $\Delta f(Z)$ curve by using KPFM [$V_{\mathrm{LCPD}}(Z)$ in Fig. 3(d)]. The SR forces obtained by the latter method and from $\Delta f(Z)$ curves produced by choosing $V_s = 180$ mV (the CPD measured 5 nm away from the surface [24]) in the $\Delta f(V_s, Z)$ maps match the ones displayed in Fig. 3(b) within the experimental error (not shown).

The similarities of the KPFM and bias-spectroscopy images shown in Fig. 1, and of the $V^*(Z)$ and $V_{\mathrm{LCPD}}(Z)$ curves displayed in Fig. 3, point toward the ac bias in KPFM having no significant influence on the measured LCPD values, since no ac bias was applied either in the bias-spectroscopy imaging or in the $\Delta f(V_s, Z)$ maps. Furthermore, the inspection of all the measured $\Delta f(V_s)$ curves obtained from the latter two methods showed no indication of a deviation from a parabolic behavior up to tip-surface separations close to the repulsive part of the SR interaction force. Thus, from the present experiments neither the application of the ac bias [16], nor the occurrence of a resonant tunneling [21] seem to be responsible for the atomic contrast in LCPD measurements at separations close to the onset of the SR interaction force.

Additionally, while there is a remarkable difference between the SR forces obtained over the Si and Pb atoms (in good agreement with previous results [35]), the differences in the LCPD curves measured over these two atomic species are very subtle. Still, a clear distinction in the onset of the drop of $V^*(Z)$ and $V_{\mathrm{LCPD}}(Z)$ can be observed [Figs. 3(c) and 3(d)], and this difference seems to be responsible for the atomic contrast in the KPFM and bias-spectroscopy images shown in Fig. 1. Moreover, the strong variation of the LCPD upon further probing the SR force suggests that the interaction with the AFM tip might have a considerable influence on the registered LCPD value; thus, care in the determination of these magnitudes has to be taken when aiming at quantitative KPFM measurements with subnanometer resolution.

In general, the work function is determined by the surface dipole [2], which is directly related to the charge distribution on the surface. To clarify a possible relation between the strong variation of the LCPD shown in Figs. 3(c) and 3(d) with possible changes in the electronic and atomic structure of the Pb/Si(111)-(7×7) surface due to the interaction with the AFM tip, we performed DFT simulations, monitoring the evolution of the surface electronic states when approaching a Si tip model over a Si and a substitutional Pb corner adatom of the Si(111)-(7×7) surface, respectively.

Our calculations show a modulation of the surface dipole orientation within the Si(111)-(7×7) unit cell in good agreement with previous experimental observations [36] (for details, see [24]). The presence of a slightly positive charged substitutional Pb adatom with a fully occupied dangling bond reduces the surface dipole moment by $\sim$0.5 D with respect to the normal surface. Upon interaction with the AFM tip, a shift in energy of the corresponding surface states similar to the one reported for a Si(111)-(7×7) surface probed with scanning tunneling microscopy [37] takes place [24].

The formation of the chemical bond between the closest tip-surface atoms also produces a local redistribution of the charge density that leads to a change of the surface dipole

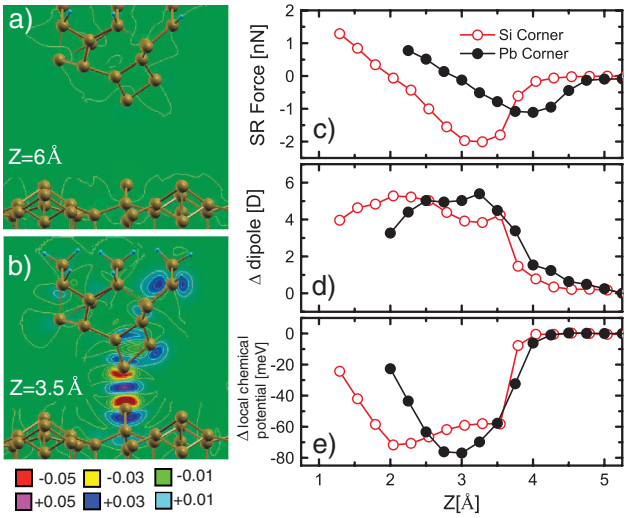

FIG. 4 (color online). Calculated differential charge density distribution ($e/\text{Å}^3$) in the real space [24], projected on a plane crossing the tip model foremost Si atom and a Si corner adatom at two relevant tip-surface separations: (a) $Z = 6$ Å and (b) $Z = 3.5$ Å. Calculated (c) short-range force, (d) change of induced surface dipole moment, and (e) variation of the local chemical potential upon approaching the tip model over a substitutional Pb and a Si corner adatom of the Pb/Si(111)-(7 × 7) surface with respect to the absence of tip interaction. Here, the local chemical potential is defined as the difference between the vacuum level and the Fermi level of the system [2].

[Fig. 4(d)], and consequently to variations of the local chemical potential [Fig. 4(e)]. This charge redistribution can be visualized by calculating the differential charge density distribution in the real space [24], projected on a plane crossing the atoms of tip and surface that are interacting [Figs. 4(a) and 4(b), and Fig. S4 in [24]]. According to our calculations, the observed change of the surface dipole amounts to ≈5 D for both Pb and Si adatoms, which corresponds to an increment in the local chemical potential of ≈80 meV [Figs. 4(d) and 4(e)]. In addition, the strong wave function overlap between tip and surface atoms established during the formation of the chemical bond increases the permittivity of the atomic contact. This effect facilitates the charge polarization across the contact due to the applied bias voltage, and consequently further increases the LCPD contrast.

Although, we obtain a reasonable agreement between theory and experiment in the distance range where changes in SR force, LCPD, and local chemical potential take place, the use of larger tip models [28,38] would provide further quantitative improvements. Additionally, we cannot exclude a change in the effective tip-sample voltage drop in the experiments due to a current flow during the tip-surface bond formation [21,39].

Work supported by the 21st Century COE program, and the MEXT of Japan. The work of P. J. was supported from Grant No. IAA100100905 and GACR No. 202/09/0545. We thank Pablo Pou and Ruben Perez for fruitful discussions.

*CUSTANCE.Oscar@nims.go.jp

[1] L. Kronik and Y. Shapira, Surf. Sci. Rep. **37**, 1 (1999).
[2] N. Lang and W. Kohn, Phys. Rev. B **3**, 1215 (1971).
[3] K. Wandelt, Appl. Surf. Sci. **111**, 1 (1997).
[4] J. Weaver *et al.* J. Vac. Sci. Technol. B **9**, 1559 (1991).
[5] W. Thomson, Philos. Mag. **46**, 82 (1898).
[6] S. Sadewasser and M. C. Lux-Steiner, Phys. Rev. Lett. **91**, 266101 (2003).
[7] Y. Rosenwaks *et al.*, Phys. Rev. B **70**, 085320 (2004).
[8] S. Siebentritt *et al.*, Phys. Rev. Lett. **97**, 146601 (2006).
[9] F. Krok *et al.*, Phys. Rev. B **77**, 235427 (2008).
[10] O. Tal *et al.*, Phys. Rev. Lett. **95**, 256405 (2005).
[11] C. Barth and C. R. Henry, Phys. Rev. Lett. **100**, 096101 (2008).
[12] U. Zerweck *et al.*, Phys. Rev. B **71**, 125424 (2005).
[13] L. Gross *et al.*, Science **324**, 1428 (2009).
[14] S. Kitamura *et al.*, Appl. Surf. Sci. **157**, 222 (2000).
[15] T. Eguchi *et al.*, Phys. Rev. Lett. **93**, 266102 (2004).
[16] K. Okamoto *et al.*, Appl. Surf. Sci. **188**, 381 (2002).
[17] G. H. Enevoldsen *et al.*, Phys. Rev. Lett. **100**, 236104 (2008).
[18] F. Bocquet *et al.*, Phys. Rev. B **78**, 035410 (2008).
[19] Here, with CPD we denote the contact potential difference registered at tip-surface separations out of the range of tip-surface interatomic forces while LCPD refers to atomic-scale variations of the CPD.
[20] L. Nony *et al.*, Phys. Rev. Lett. **103**, 036802 (2009).
[21] T. Arai and M. Tomitori, Phys. Rev. Lett. **93**, 256101 (2004).
[22] T. R. Albrecht *et al.*, J. Appl. Phys. **69**, 668 (1991).
[23] I. Horcas *et al.*, Rev. Sci. Instrum. **78**, 013705 (2007).
[24] See EPAPS Document No. E-PRLTAO-104-015001 for additional information. For more information on EPAPS, see http://www.aip.org/pubservs/epaps.html.
[25] M. Guggisberg *et al.*, Phys. Rev. B **61**, 11 151 (2000).
[26] M. A. Lantz *et al.*, Science **291**, 2580 (2001).
[27] J. E. Sader *et al.*, Appl. Phys. Lett. **84**, 1801 (2004).
[28] P. Pou *et al.*, Nanotechnology **20**, 264015 (2009).
[29] P. Jelinek *et al.*, Phys. Rev. B **71**, 235101 (2005).
[30] We have performed numerous experiments in different sessions yielding to similar results. In this Letter we publish exemplary data from one of these sessions.
[31] S. Kitamura *et al.*, Jpn. J. Appl. Phys. **44**, 8113 (2005).
[32] Our DFT results show that the Pb adatoms protrude from the surface plane. This accounts for their higher contrast in topography in spite of the fact that the tip-surface interatomic force over the Si adatoms is stronger.
[33] Our DFT calculations reproduce this behavior.
[34] We have observed variability in the measurement of the LCPD, with some tip-apex terminations producing atomic contrast in topography but yielding to a flat contrast in both KPFM and bias-spectroscopy images.
[35] Y. Sugimoto *et al.*, Nature (London) **446**, 64 (2007).
[36] Y. Cho and R. Hirose, Phys. Rev. Lett. **99**, 186101 (2007).
[37] P. Jelínek *et al.*, Phys. Rev. Lett. **101**, 176101 (2008).
[38] L. Nony *et al.*, Nanotechnology **20**, 264014 (2009).
[39] D. Sawada *et al.*, Appl. Phys. Lett. **94**, 173117 (2009).